Journal of Science and Technology in Civil Engineering NUCE 2019. 13 (1): 33–45

BENDING ANALYSIS OF FUNCTIONALLY GRADED BEAM WITH POROSITIES RESTING ON ELASTIC FOUNDATION BASED ON NEUTRAL SURFACE POSITION

Nguyen Thi Bich Phuong[a,*], Tran Minh Tu[a], Hoang Thu Phuong[a], Nguyen Van Long[b]

[a] *Faculty of Building and Industrial Construction, National University of Civil Engineering, 55 Giai Phong road, Hai Ba Trung district, Hanoi, Vietnam*
[b] *Construction Technical College No. 1, Trung Van, Tu Liem, Hanoi, Vietnam*

Article history:
Received 10 December 2018, Revised 28 December 2018, Accepted 24 January 2019

Abstract

In this paper, the Timoshenko beam theory is developed for bending analysis of functionally graded beams having porosities. Material properties are assumed to vary through the height of the beam according to a power law. Due to unsymmetrical material variation along the height of functionally graded beam, the neutral surface concept is proposed to remove the stretching and bending coupling effect to obtain an analytical solution. The equilibrium equations are derived using the principle of minimum total potential energy and the physical neutral surface concept. Navier-type analytical solution is obtained for functionally graded beam subjected to transverse load for simply supported boundary conditions. The accuracy of the present solutions is verified by comparing the obtained results with the existing solutions. The influences of material parameters (porosity distributions, porosity coefficient, and power-law index), span-to-depth ratio and foundation parameter are investigated through numerical results.

Keywords: functionally graded beam; bending analysis; porosity; elastic foundation; bending; neutral surface.

https://doi.org/10.31814/stce.nuce2019-13(1)-04

1. Introduction

Functionally graded materials (FGMs) are novel generation of composites that have a continuous variation of material properties from one surface to another. The earliest FGMs were introduced by Japanese scientists in mid-1984 as thermal barrier materials for applications in spacecraft, space structures and nuclear reactors. FGMs can be fabricated by gradually varying the volume fraction of the constituent materials. Typically, FGMs are made of a combination of ceramics and different metals. The gradation in the properties of the materials reduces thermal stresses, residual stresses and stress concentration factors found in laminated and fiber-reinforced composites.

Recently, a lot of research on the dynamic and static analysis of functionally graded beams (FG beams) have been conducted. Vo et al. [1] presented static and vibration analysis of functionally graded beams using refined shear deformation theory, which does not require shear correction factor, accounting for shear deformation effect and coupling coming from the material anisotropy. Using the spectral finite element method, Chakraborty and Gopalakrishnan [2] studied wave propagation in FG beams. Sankar [3] found out an elasticity solution for bending of FG beams using Euler–Bernoulli

*Corresponding author. *E-mail address:* phuongce710@gmail.com (Phuong, N. T. B.)

beam theory, in which Poisson's ratio was considered to be constant, and Young's modulus was assumed to vary following an exponential function. Zhong and Yu [4] employed the Airy stress function to develop an analytical solution for cantilever beams subjected to various types of mechanical loadings. The bending response of FG beams with higher order shear deformation was also investigated by Kadoli et al. [5].

Due to micro voids or porosities occurring inside FGMs during fabrication, structures with graded porosity can be introduced as one of the latest development in FGMs. When designing and analyzing FG structures, it is important to take into consideration the porosity effect. Wattanasakulpong and Ungbhakorn [6] investigated linear and nonlinear vibration characteristics of Euler FG beams with porosities. The beams are assumed to be supported by elastic boundary conditions. Atmane et al. [7] presented a free vibrational analysis of FG beams considering porosities using computational shear displacement model. Vibration characteristics of Reddy's FG beams with porosity effect and various thermal loadings are investigated by Ebrahimi and Jafari [8]. Ebrahimi et al. [9] analyzed vibration characteristics of temperature-dependent FG Euler's beams with porosity considering the effect of uniform, linear and nonlinear temperature distribution.

In FG beams, the material characteristics vary across the height direction. Therefore, the neutral surface of the beams may not coincide with their geometric mid-surface. As a result, stretching and bending deformations of FG beams are coupled. In this aspect, some studies [10–12] have shown that there is no stretching-bending coupling in the constitutive equations if the reference surface is selected accurately. Recently, Bouremana et al. [13] developed a new first shear deformation beam theory based on neutral surface position for FG beams. A novel shear deformation beam theory for FG beams including the so-called "stretching effect" was proposed by Meradjah et al. [14].

In this paper, the Timoshenko beam theory for FG beams having porosities is used to derive the equations of motion based on the exact position of neutral surface together with principle of minimum total potential energy. Two types of porosity distributions, namely even and uneven through the height directions are considered. Numerical results indicate that various parameters such as power-law indices, porosity coefficient and types of porosity distribution have remarkable influence on deflections and stresses of FG beams with porosities.

2. Theoretical formulations

2.1. Physical neutral surface [10]

In this study, the imperfect FG beam is made up of a mixture of ceramic and metal and the properties are assumed to vary through the height of the beam according to power law. The top surface material is ceramic-rich and the bottom surface material is metal-rich. The imperfect beam is assumed to have porosities spreading throughout its height due to defect during fabrication. For such beams, the neutral surface may not coincide with its geometric midsurface. The coordinates x, y are along the in-plane directions and z is along the height direction. To specify the position of neutral surface of FG beams, two different planes are considered for the measurement of z, namely, z_{ms} and z_{ns} measured from the middle surface and the neutral surface of the beam, respectively, as depicted in Fig. 1. It is assumed that the beam is rested on a Pasternak elastic foundation with the Winkler stiffness of K_w and shear stiffness of K_s.

The effective material properties of imperfect FG beam with two kinds of porosities distributed identically in two phases of ceramic and metal can be expressed using the modified rule of mixture.

In this study, the neutral surface is chosen as a reference plane. The imperfect FGM has been studied with two types of porosity distributions (even and uneven) across the beam height due to

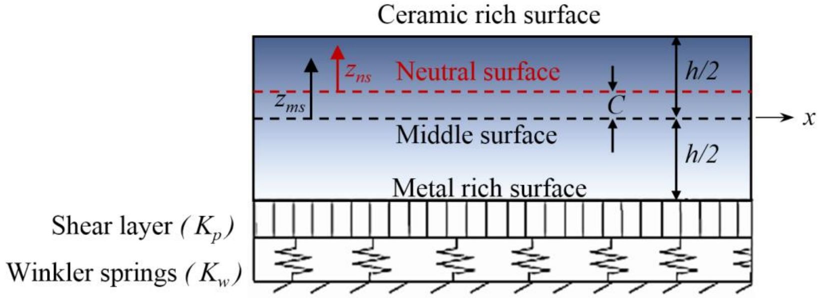

Figure 1. The position of middle surface and neutral surface for a FG beam resting on the Pasternak elastic foundation

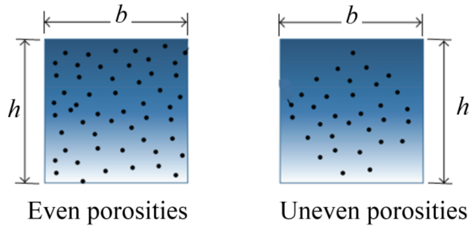

Figure 2. Cross-sectional area of FGM beam with even and uneven porosities

defect during fabrication. As can be seen from Fig. 2, the first type (FGM-I) has porosity phases with even distribution of volume fraction over the cross section, while the second type (FGM-II) has porosity phases spreading more frequently near the middle zone of the cross section and the amount of porosity seems to linearly decrease to zero at the top and bottom of the cross section.

Thus, for even distribution of porosities (FGM-I), the effective material properties of the imperfect FG beam are obtained as follows [9]:

$$P = P_m\left(V_m - \frac{e_0}{2}\right) + P_c\left(V_c - \frac{e_0}{2}\right) \tag{1}$$

where e_0 denotes the porosity coefficient, ($e_0 \ll 1$) , the material properties of a perfect FG beam can be obtained when e is set to zero. P_c and P_m are the material properties of ceramic and metal such as: Young's modulus E, mass density ρ; V_c and V_m are the volume fraction of the ceramic and the metal constituents, related by:

$$V_m + V_c = 1 \tag{2}$$

The volume fraction of the ceramic constituent V_c is expressed based on z_{ms} and z_{ns} coordinates as

$$V_c = \left(\frac{z_{ms}}{h} + \frac{1}{2}\right)^p = \left(\frac{z_{ns} + C}{h} + \frac{1}{2}\right)^p \tag{3}$$

From Eqs. (1) and (3), the effective material properties of the imperfect FG beam with even distribution of porosities (FGM-I) are expressed as [9]

$$P(z_{ns}) = P_m + (P_c - P_m)\left(\frac{z_{ns} + C}{h} + \frac{1}{2}\right)^p - (P_c + P_m)\,\frac{e_0}{2} \tag{4}$$

where p is the power law index, which is greater or equal to zero, and C is the distance of neutral surface from the mid-surface. The FG beam becomes a fully ceramic beam when p is set to zero and fully metal for large value of p.

For the uneven distribution of porosities (FGM-II), the effective material properties of the imperfect FG beam are replaced by following form [9]:

$$P(z_{ns}) = P_m + (P_c - P_m)\left(\frac{z_{ns} + C}{h} + \frac{1}{2}\right)^p - (P_c + P_m)\,\frac{e_0}{2}\left(1 - \frac{2\,|z_{ns} + C|}{h}\right) \tag{5}$$

The position of the neutral surface of the FG beam is determined to satisfy the first moment with respect to Young's modulus being zero as follows [15]:

$$\int\limits_{-h/2}^{h/2} E(z_{ms})\,(z_{ms} - C)\,dz_{ms} = 0 \tag{6}$$

Consequently, the position of neutral surface can be obtained as:

$$C = \frac{\int\limits_{-h/2}^{h/2} E(z_{ms}) z_{ms} dz_{ms}}{\int\limits_{-h/2}^{h/2} E(z_{ms}) dz_{ms}} \tag{7}$$

From Eqs. (7), it can be seen that the parameter C is zero for homogeneous isotropic beams as expected.

2.2. Kinematics and constitutive equations

Using the physical neutral surface concept and Timoshenko beam theory (TBT), the displacements take the following forms [15–18]:

$$\begin{aligned} u(x, z_{ns}) &= u_0(x) + z_{ns}\theta_x(x) \\ w(x, z_{ns}) &= w_0(x) \end{aligned} \tag{8}$$

where u_0 and w_0 denote the displacements at the neutral surface of plate in the x and z directions, respectively; θ_x is the rotation of the cross-section of the beam.

Then, the nonzero strains displacement relation of Timoshenko beam theory can be expressed as follows:

$$\begin{aligned} \varepsilon_{xx} &= \frac{\partial u}{\partial x} = \frac{\partial u_0}{\partial x} + z_{ns}\frac{\partial \theta_x}{\partial x} = \varepsilon^0_{xx} + z_{ns}\kappa^0_{xx} \\ \gamma_{xz} &= \frac{\partial w}{\partial x} + \frac{\partial u}{\partial z} = \frac{\partial w_0}{\partial x} + \theta_x = \gamma^0_{xz} \end{aligned} \tag{9a}$$

where

$$\varepsilon^0_{xx} = \frac{\partial u_0}{\partial x}; \quad \kappa^0_{xx} = \frac{\partial \theta_x}{\partial x}; \quad \gamma^0_{xx} = \frac{\partial w_0}{\partial x} + \theta_x \tag{9b}$$

The constitutive relations of the beam can be expressed using the generalized Hooke's law as follows:

$$\begin{aligned} \sigma_{xx} &= Q_{11}(z_{ns})\varepsilon_{xx} \\ \tau_{xz} &= Q_{55}(z_{ns})\gamma_{xz} \end{aligned} \tag{10}$$

where

$$Q_{11}(z_{ns}) = E(z_{ns}); \quad Q_{55}(z_{ns}) = \frac{E(z_{ns})}{2\,[1 + \nu(z_{ns})]} \tag{11}$$

2.3. Equilibrium equations

The equilibrium equations and boundary conditions can be obtained using the principle of minimum total potential energy [19, 20], i.e.,

$$\delta (U + V) = 0 \tag{12}$$

where δU is the variation of the strain energy of the beam-foundation system and δV is the variation of the potential energy of external loads.

The variation of the strain energy of the beam is:

$$\begin{aligned}
\delta U &= \int_0^L \int_A (\sigma_{xx}\delta\varepsilon_x + \tau_{xz}\delta\gamma_{xz})\, dA dx + \int_0^L \left(K_w w \delta w - K_s \frac{\partial^2 w}{\partial x^2}\delta w\right) dx \\
&= \int_0^L \left(N_{xx}\delta\varepsilon^0_{xx} + M_{xx}\delta\kappa^0_{xx} + Q_{xz}\delta\gamma^0_{xz}\right) dx + \int_0^L \left(K_w w_0 \delta w_0 - K_s \frac{\partial^2 w_0}{\partial x^2}\delta w_0\right) dx \\
&= \int_0^L \left[N_{xx}\frac{\partial \delta u_0}{\partial x} + M_{xx}\frac{\partial \delta\theta_x}{\partial x} + Q_{xz}\left(\frac{\partial \delta w_0}{\partial x} + \delta\theta_x\right)\right] dx + \int_0^L \left(K_w w_0 \delta w_0 - K_s \frac{\partial^2 w_0}{\partial x^2}\delta w_0\right) dx
\end{aligned} \tag{13}$$

where N_{xx}, M_{xx}, and Q_{xz} are the stress resultants defined as:

$$\begin{aligned}
N_{xx} &= \int_A \sigma_{xx} dA = A_{11}\frac{\partial u_0}{\partial x} + B_{11}\frac{\partial \theta_x}{\partial x} \\
M_{xx} &= \int_A \sigma_{xx} z dA = B_{11}\frac{\partial u_0}{\partial x} + D_{11}\frac{\partial \theta_x}{\partial x} \\
Q_{xz} &= k_s \int_A \sigma_{xz} dA = A^s_{55}\left(\frac{\partial w_0}{\partial x} + \theta_x\right)
\end{aligned} \tag{14}$$

in which

$$\begin{aligned}
A_{11} &= \int_A Q_{11}(z_{ns}) dA = b \int_{-h/2-C}^{h/2-C} E(z_{ns}) dz_{ns} \\
&= b \int_{-h/2-C}^{h/2-C} E(z_{ns}) dz_{ns} = b \int_{-h/2}^{h/2} E(z_{ms}) dz_{ms} \\
B_{11} &= \int_A z_{ns} Q_{11}(z_{ns}) dA = b \int_{-h/2-C}^{h/2-C} z_{ns} E(z_{ns}) dz_{ns} = 0 \\
&= b \int_{-h/2-C}^{h/2-C} z_{ns} E(z_{ns}) dz_{ns} = b \int_{-h/2}^{h/2} (z_{ms} - C)\, E(z_{ms}) dz_{ms} \\
&= b \int_{-h/2}^{h/2} z_{ms} E(z_{ms}) dz_{ms} - Cb \int_{-h/2}^{h/2} E(z_{ms}) dz_{ms} = 0
\end{aligned} \tag{15}$$

$$D_{11} = \int_A z_{ns}^2 Q_{11}(z_{ns}) dA = b \int_{-h/2-C}^{h/2-C} z_{ns}^2 E(z_{ns}) dz_{ns}$$

$$A_{55}^s = k_s \int_A Q_{55}(z_{ns}) dA = bk_s \int_{-h/2-C}^{h/2-C} \frac{E(z_{ns})}{2\left[1-\nu(z_{ns})\right]} dz_{ns}$$

The shear correction factor $k_s = \dfrac{5}{6}$ is used in this study.

Substituting (15) into Eq. (14), the stress resultants for the imperfect FG beam can be rewritten as:

$$\begin{aligned} N_{xx} &= A_{11}\frac{\partial u_0}{\partial x} \\ M_{xx} &= D_{11}\frac{\partial \theta_x}{\partial x} \\ Q_{xz} &= A_{55}^s\left(\frac{\partial w_0}{\partial x} + \theta_x\right) \\ M_{xx} &= D_{11}\frac{\partial \theta_x}{\partial x} \\ Q_{xz} &= A_{55}^s\left(\frac{\partial w_0}{\partial x} + \theta_x\right) \end{aligned} \tag{16}$$

The variation of the potential energy by the applied transverse load q can be expressed as:

$$\delta V = -\int_0^L q\delta w_0 dx \tag{17}$$

Substituting the expressions for δU and δV from Eqs. (13), and (17) considering Eq. (18) into Eq. (12) and integrating by parts, we obtain:

$$\begin{aligned} 0 &= \int_0^L \left[N_{xx}\frac{\partial \delta u_0}{\partial x} + M_{xx}\frac{\partial \delta\theta_x}{\partial x} + Q_{xz}\left(\frac{\partial \delta w_0}{\partial x} + \delta\theta_x\right)\right] dx \\ &+ \int_0^L \left(K_w w_0 \delta w_0 - K_s\frac{\partial^2 w_0}{\partial x^2}\delta w_0\right) dx - \int_0^L q\delta w_0 dx \\ 0 &= N_{xx}\delta u_0\Big|_0^L + M_{xx}\delta\theta_x\Big|_0^L + Q_{xz}\delta w_0\Big|_0^L \\ &- \int_0^L \left[\frac{\partial N_{xx}}{\partial x}\delta u_0 + \left(\frac{\partial M_{xx}}{\partial x} - Q_{xz}\right)\delta\theta_x + \left(\frac{\partial Q_{xz}}{\partial x} + q - K_w w_0 + K_s\frac{\partial^2 w_0}{\partial x^2}\right)\delta w_0\right] dx \end{aligned} \tag{18}$$

Collecting the coefficients of $\delta u_0, \delta w_0$ and $\delta\theta_x$, the following equilibrium equations of the FG beam are obtained as follows:

$$\begin{aligned} \delta u_0 &: \frac{\partial N_{xx}}{\partial x} = 0 \\ \delta w_0 &: \frac{\partial Q_{xz}}{\partial x} + q - K_w w_0 + K_s \frac{\partial^2 w_0}{\partial x^2} = 0 \\ \delta \theta_x &: \frac{\partial M_{xx}}{\partial x} - Q_{xz} = 0 \end{aligned} \tag{19}$$

The force (natural) boundary conditions for the Timoshenko beam theory involve specifying the following secondary variables:

$$N_{xx}, Q_{xz} \quad \text{and} \quad M_{xx} \quad \text{at} \quad x = 0, L \tag{20a}$$

The geometric boundary conditions involve specifying the following primary variables:

$$u_0, w_0 \quad \text{and} \quad \theta_x \quad \text{at} \quad x = 0, L \tag{20b}$$

Thus, the pairing of the primary and secondary variables is as follows:

$$(u_0, N_{xx}), \ (w_0, Q_{xz}), (\theta_x, M_{xx}) \tag{20c}$$

Only one member of each pair may be specified at a point in the beam.

2.4. Equilibrium equations in terms of displacements

By substituting the stress resultants in Eq. (16) into Eq. (19), the equilibrium equations can be expressed in terms of displacements (u_0, w_0, θ_x) as:

$$A_{11} \frac{\partial^2 u_0}{\partial x^2} = 0 \tag{21a}$$

$$A_{55}^s \frac{\partial^2 w_0}{\partial x^2} + A_{55}^s \frac{\partial \theta_x}{\partial x} + q - K_w w_0 + K_s \frac{\partial^2 w_0}{\partial x^2} = 0 \tag{21b}$$

$$D_{11} \frac{\partial^2 \theta_x}{\partial x^2} - A_{55}^s \frac{\partial w_0}{\partial x} - A_{55}^s \theta_x = 0 \tag{21c}$$

3. The Navier solution

The simply supported boundary conditions of FG beams are:

$$w_0 = 0, \ N_{xx} = 0, \ M_{xx} = 0 \quad \text{at} \quad x = 0, L \tag{22}$$

The above equilibrium equations are analytically solved for bending problems. The Navier solution procedure is used to determine the analytical solutions for a simply supported beam. The solution is assumed to be of the form:

$$u_0(x,t) = \sum_{m=1}^{\infty} u_{0m} \cos \alpha x; w_0(x,t) = \sum_{m=1}^{\infty} w_{0m} \sin \alpha x; \theta_x(x,t) = \sum_{m=1}^{\infty} \theta_{xm} \cos \alpha x \tag{23}$$

where $\alpha = \dfrac{m\pi}{L}$; m is the half wave number in the x direction; $(u_{0m}, w_{0m}, \theta_{xm})$ are the unknown maximum displacement coefficients.

The transverse load q is also expanded in Fourier series as:

$$q(x) = \sum_{m=1}^{\infty} q_m \sin \alpha x \tag{24a}$$

where q_m is the load amplitude calculated from:

$$q_m = \frac{2}{L} \int_0^L q(x) \sin \alpha x dx \tag{24b}$$

The coefficients q_m are given below for some typical loads:

$$q_m = q_0 \quad \text{for sinusoidal load } (m = 1) \tag{24c}$$

$$q_m = \frac{4q_0}{\pi m} \quad \text{for uniform load} \tag{24d}$$

Substituting the expansions of u_0, w_0, θ_x and q from Eqs. (23) and (24) into Eq. (21) and collecting the coefficients, we obtain a 3×3 system of equations:

$$\begin{bmatrix} s_{11} & 0 & 0 \\ 0 & s_{22} & s_{23} \\ 0 & s_{32} & s_{33} \end{bmatrix} \begin{Bmatrix} u_{0m} \\ w_{0m} \\ \theta_{xm} \end{Bmatrix} = \begin{Bmatrix} 0 \\ q_m \\ 0 \end{Bmatrix} \tag{25}$$

for any fixed values of m and n.

In which:

$$s_{11} = A_{11}\alpha^2; \quad s_{22} = \left(A_{55}^s + K_s\right)\alpha^2 + K_w; \quad s_{23} = s_{32} = A_{55}^s\alpha; \quad s_{33} = D_{11}\alpha^2 + A_{55}^s$$

The analytical solutions can be obtained from Eqs. (25), and are expressed in the following form:

$$u_{0m} = 0; w_{0m} = \frac{s_{33}q_m}{s_{22}s_{33} - s_{23}^2}; \quad \theta_{xm} = \frac{-s_{23}q_m}{s_{22}s_{33} - s_{23}^2} \tag{26}$$

or

$$\begin{aligned} u_{0m} &= 0 \\ w_{0m} &= \frac{\left(D_{11}\alpha^2 + A_{55}^s\right)q_m}{A_{55}^s D_{11}\alpha^4 + \left(K_s\alpha^2 + K_w\right)\left(D_{11}\alpha^2 + A_{55}^s\right)} \\ \theta_{xm} &= \frac{-A_{55}^s\alpha q_m}{A_{55}^s D_{11}\alpha^4 + \left(K_s\alpha^2 + K_w\right)\left(D_{11}\alpha^2 + A_{55}^s\right)} \end{aligned} \tag{27}$$

4. Results and discussion

In the following section, after validation of the analytical solution based on neutral surface concept, the influence of different beam parameters such as porosity distribution, porosity volume fraction, power law exponent, and slenderness on the deflection and stress components of the imperfect FG beam under uniform, and sinusoidal distributed loading will be perceived.

The FG beams are made of aluminum (Al; E_m = 70 GPa, ν_m = 0.3) and alumina (Al_2O_3; E_c = 380 GPa, ν_c = 0.3) and their properties vary throughout the height of the beam according to power-law. For convenience, the following dimensionless forms are used [21]:

$$\bar{w}\left(L/2\right) = 100w\left(L/2\right)\frac{E_c I}{q_0 L^4}; \quad \bar{K}_w = K_w \frac{L^4}{EI}; \quad \bar{K}_s = K_s \frac{L^2}{EI} \tag{28}$$

where $I = \dfrac{bh^3}{12}$ is the second moment of the cross-sectional area.

Table 1 presents the comparisons of the non dimensional mid-span deflection $\bar{w}\left(L/2\right)$ obtained from the present analytical solution based on neutral surface concept with results of Chen et al. [22], Ying et al. [23] using two-dimensional elasticity solution for two various values of height-to-length ratio, and for different values of foundation parameters $\bar{K}_w$ and $\bar{K}_s$. As can be seen, the present results are in good agreement with previous ones

Table 1. Comparisons of the mid-span deflection $\bar{w}\left(L/2\right)$ of an isotropic homogeneous beam on elastic foundations due to uniform pressure

Foundation parameters		$L/h = 120$			$L/h = 5$		
$\bar{K}_w$	$\bar{K}_s$	Ying et al. [23]	Chen et al. [22]	Present	Ying et al. [23]	Chen et al. [22]	Present
0	0	1.3023	1.3023	1.3023	1.4202	1.4203	1.4321
10	0	1.1806	1.1794	1.1806	1.2773	1.2826	1.2855
	10	0.6133	0.6133	0.6133	0.6403	0.6464	0.6387
	25	0.3557	0.3557	0.3557	0.3657	0.3721	0.3631
100	0	0.6401	0.6401	0.6401	0.6685	0.6961	0.6671
	10	0.4256	0.4256	0.4256	0.4388	0.4593	0.4362
	25	0.2829	0.2828	0.2828	0.2894	0.3052	0.2869

Table 2 contains the nondimensional deflections of perfect and imperfect FG beams under uniform and sinusoidal distributed load for different values of power law index p (span-to-depth ratio L/h = 10, porosity coefficient $e_0 = 0.1$; $\bar{K}_w = 100$, $\bar{K}_p = 10$). The results obtained for perfect FGM ($e_0 = 0$), even distribution of porosities (FGM-I), and uneven distribution of porosities (FGM-II).

Fig. 3 presents the variation of the non-dimensional deflections versus power law index p for three types of porosity distribution. It can be deduced from this curve that the higher the power law index is, the higher the deflection is, regardless the type of loading. So, by increasing the metal percentage and decreasing the value of Young's modulus in metal with respect to ceramic, the stiffness of the system decreases. Besides, it is found that the nondimensional deflection of porous FG beams with evenly distributed porosity (FGM-I) is lower than the FG beam with uneven distributed porosity (FGM-II), and the nondimensional deflection of perfect FG beam is the lowest.

In Table 3, maximum non-dimensional deflections of the beam are presented for various values of span-to-depth ratios L/h and different types of porous FG beams under uniform load. Table 4 shows the maximum nondimensional deflections of perfect and imperfect FG beams under uniform load for different values of porosity coefficients.

Fig. 4 depicts the variation of maximum non-dimensional transverse deflection of the different types of FG beams versus span-to-depth ratios and porosity coefficients. It can be observed that the

Table 2. Nondimensional deflections of FG beams under uniform and sinusoidal distributed load for different values of power law index p $\left(L/h = 10, e_0 = 0.1, \bar{K}_w = 100, \bar{K}_s = 10\right)$

Loading	Materials	p					
		0	0.5	1	2	5	10
UL	FGM	0.4283	0.4815	0.5081	0.5292	0.5414	0.5475
	FGM-I	0.4365	0.4925	0.5213	0.5449	0.5578	0.5625
	FGM-II	0.4304	0.4844	0.5118	0.5339	0.5463	0.5517
SL	FGM	0.3405	0.3840	0.4061	0.4241	0.4349	0.4405
	FGM-I	0.3471	0.3930	0.4173	0.4377	0.4495	0.4541
	FGM-II	0.3422	0.3864	0.4093	0.4282	0.4393	0.4443

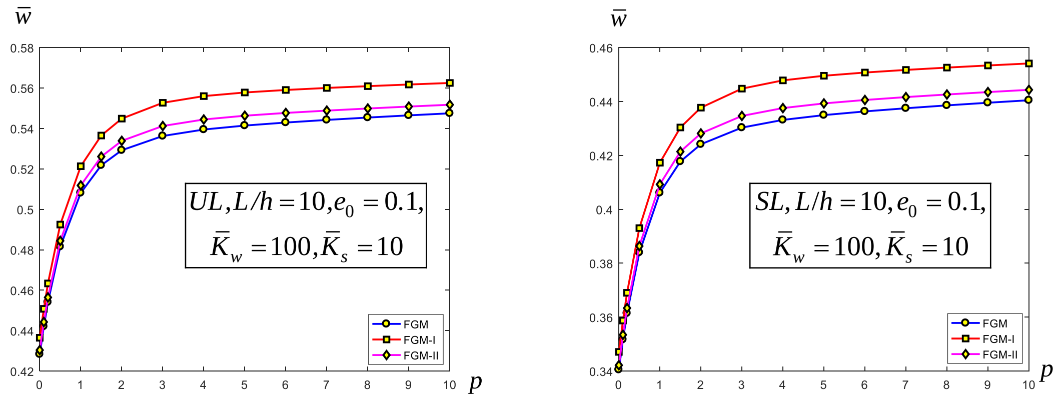

Figure 3. Variation of nondimensional transverse deflection $\bar{w}\,(L/2)$ with respect to the power law index p for imperfect FG beams under uniform (UL) and sinusoidal distributed (SL) load

Table 3. Maximum non-dimensional transverse deflection of the FG beam for various values of span-to-depth ratios L/h $\left(p = 2, e_0 = 0.1, \bar{K}_w = 100, \bar{K}_s = 10\right)$

Materials	L/h					
	5	10	15	20	25	30
FGM	0.5315	0.5292	0.5288	0.5287	0.5286	0.5286
FGM-I	0.5460	0.5449	0.5447	0.5446	0.5446	0.5446
FGM-II	0.5358	0.5339	0.5335	0.5334	0.5334	0.5334

maximum nondimensional transverse deflection decreases with increasing span-to-depth ratio, and decreases significantly in range of L/h from 5 to 15. Also, it is concluded that increasing porosity coefficient increases maximum nondimensional transverse deflection. Thus, as also known from mechanical behavior of the beam, the deflection increases as the flexibility of a structure increases. Furthermore, existence of porosity will cause a decrease of stiffness of the structure. In FGM I (even distribution) the porosity has more significant impact on the non-dimensional deflection of FG beam than that of FGM II (uneven distribution).

Maximum non-dimensional transverse deflections of the perfect and imperfect FG beams for

Table 4. Maximum non-dimensional transverse deflection of the beam for various values of porosity coefficients $\left(p = 2, L/h = 10, \bar{K}_w = 100, \bar{K}_s = 10\right)$

Materials	α					
	0	0.05	0.1	0.15	0.2	0.3
FGM	0.5292	0.5292	0.5292	0.5292	0.5292	0.5292
FGM-I	0.5292	0.5368	0.5449	0.5533	0.5624	0.5823
FGM-II	0.5292	0.5315	0.5339	0.5363	0.5388	0.5442

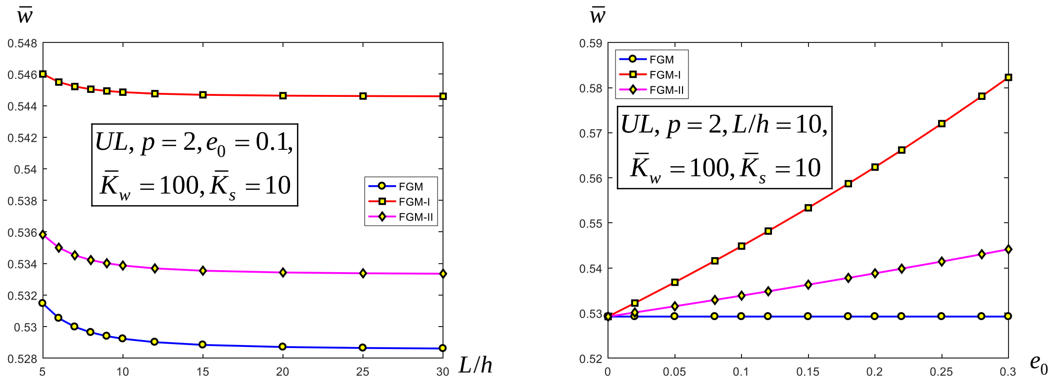

Figure 4. Variation of nondimensional transverse deflection $\bar{w}\,(L/2)$ with respect to the span-to-depth ratio L/h and with respect to porosity coefficient for imperfect FG beams under uniform load

various values of Winkler foundation parameters, and for various values of Pasternak foundation parameters are tabulated in Tables 5 and 6.

The variations of the maximum non-dimensional transverse deflections versus the foundation parameter are plotted in Fig. 5. It can be deduced from these plots that the higher the Winkler (or Pasternak) foundation parameter is, the lower the transverse deflection is, regardless of the type of FG beams. This is because the beam gets stiffer with increasing foundation parameters (Winkler and Pasternak).

Table 5. Maximum non-dimensional transverse deflection of the FG beam for various values of Winkler foundation parameters $\left(\bar{K}_s = 0; p = 2, L/h = 10, e_0 = 0.1\right)$

Materials	$\bar{K}_w$					
	0	10	50	100	200	300
FGM	3.4190	2.6896	1.4473	0.9143	0.5230	0.3642
FGM-I	4.2588	3.1832	1.5780	0.9634	0.5372	0.3699
FGM-II	3.6359	2.8219	1.4845	0.9286	0.5273	0.3660

Table 6. Maximum non-dimensional transverse deflection of the FG beam for various values of Pasternak foundation parameters $\left(\bar{K}_w = 0; p = 2, L/h = 10, e_0 = 0.1\right)$

Materials	$\bar{K}_s$					
	0	5	10	15	20	25
FGM	0.9143	0.6706	0.5292	0.4370	0.3721	0.3240
FGM-I	0.9634	0.6962	0.5449	0.4475	0.3796	0.3296
FGM-II	0.9286	0.6781	0.5339	0.4401	0.3744	0.3257

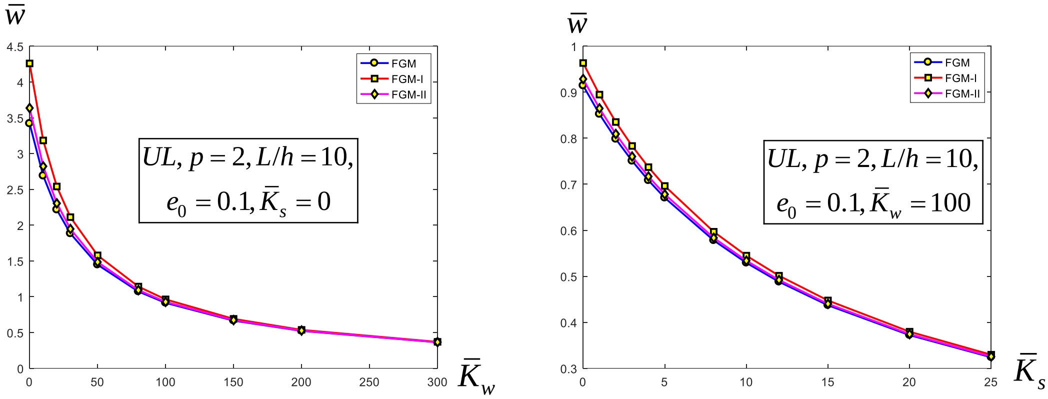

Figure 5. Variation of the maximum non-dimensional transverse displacement of FG beam with Winkler foundation parameter $\bar{K}_w$ and Pasternak shear foundation parameter $\bar{K}_s$

5. Summary and conclusions

In this paper, the Timoshenko beam theory based on neutral surface position is used for bending analysis of functionally graded perfect and imperfect beams resting on Winkler-Pasternak elastic foundation. Thus, membrane force and bending moment have no stretching–bending couplings, and governing equations have simple forms, so the solution procedure is similar to that of homogeneous isotropic beam.

The effective material properties are assumed to vary continuously in the height direction of the beam according to the rule of mixture, which is reformulated to assess the material characteristics with the porosity phases. The governing differential equations and related boundary conditions are derived by implementing the principle of minimum total potential energy. The Navier-type solution is used for simply-supported boundary conditions, and exact formulas are proposed for the static deflections. Accuracy of the results is examined using available data in the literature. Numerical results show that the porosity distributions, porosity coefficient, power-law index and foundation parameter play a major role on the static response of the FG beam. In the design of functionally graded structures, by choosing a suitable power-law index, the material properties of the FG beam can be tailored to meet the desired goals of minimizing stresses and displacements in a beam-type structure.

References

[1] Vo, T. P., Thai, H.-T., Nguyen, T.-K., Inam, F. (2014). Static and vibration analysis of functionally graded beams using refined shear deformation theory. *Meccanica*, 49(1):155–168.

[2] Chakraborty, A., Gopalakrishnan, S. (2003). A spectrally formulated finite element for wave propagation analysis in functionally graded beams. *International Journal of Solids and Structures*, 40(10):2421–2448.
[3] Sankar, B. V. (2001). An elasticity solution for functionally graded beams. *Composites Science and Technology*, 61(5):689–696.
[4] Zhong, Z., Yu, T. (2007). Analytical solution of a cantilever functionally graded beam. *Composites Science and Technology*, 67(3-4):481–488.
[5] Kadoli, R., Akhtar, K., Ganesan, N. (2008). Static analysis of functionally graded beams using higher order shear deformation theory. *Applied Mathematical Modelling*, 32(12):2509–2525.
[6] Wattanasakulpong, N., Ungbhakorn, V. (2014). Linear and nonlinear vibration analysis of elastically restrained ends FGM beams with porosities. *Aerospace Science and Technology*, 32(1):111–120.
[7] Atmane, H. A., Tounsi, A., Bernard, F., Mahmoud, S. (2015). A computational shear displacement model for vibrational analysis of functionally graded beams with porosities. *Steel and Composite Structures*, 19 (2):369–384.
[8] Ebrahimi, F., Jafari, A. (2016). A higher-order thermomechanical vibration analysis of temperature-dependent FGM beams with porosities. *Journal of Engineering*, 2016.
[9] Ebrahimi, F., Ghasemi, F., Salari, E. (2016). Investigating thermal effects on vibration behavior of temperature-dependent compositionally graded Euler beams with porosities. *Meccanica*, 51(1):223–249.
[10] Larbi, L. O., Kaci, A., Houari, M. S. A., Tounsi, A. (2013). An efficient shear deformation beam theory based on neutral surface position for bending and free vibration of functionally graded beams. *Mechanics Based Design of Structures and Machines*, 41(4):421–433.
[11] Yaghoobi, H., Fereidoon, A. (2010). Influence of neutral surface position on deflection of functionally graded beam under uniformly distributed load. *World Applied Sciences Journal*, 10(3):337–341.
[12] Bourada, M., Kaci, A., Houari, M. S. A., Tounsi, A. (2015). A new simple shear and normal deformations theory for functionally graded beams. *Steel and Composite Structures*, 18(2):409–423.
[13] Bouremana, M., Houari, M. S. A., Tounsi, A., Kaci, A., Bedia, E. A. A. (2013). A new first shear deformation beam theory based on neutral surface position for functionally graded beams. *Steel and Composite Structures*, 15(5):467–479.
[14] Meradjah, M., Kaci, A., Houari, M. S. A., Tounsi, A., Mahmoud, S. R. (2015). A new higher order shear and normal deformation theory for functionally graded beams. *Steel and Composite Structures*, 18(3): 793–809.
[15] Zhang, D.-G., Zhou, Y.-H. (2008). A theoretical analysis of FGM thin plates based on physical neutral surface. *Computational Materials Science*, 44(2):716–720.
[16] Xiang, H. J., Yang, J. (2008). Free and forced vibration of a laminated FGM Timoshenko beam of variable thickness under heat conduction. *Composites Part B: Engineering*, 39(2):292–303.
[17] Reddy, J. N. (2006). *Theory and analysis of elastic plates and shells*. CRC press.
[18] She, G.-L., Yuan, F.-G., Ren, Y.-R. (2017). Thermal buckling and post-buckling analysis of functionally graded beams based on a general higher-order shear deformation theory. *Applied Mathematical Modelling*, 47:340–357.
[19] Reddy, J. N. (2017). *Energy principles and variational methods in applied mechanics*. John Wiley & Sons.
[20] Dym, C. L., Shames, I. H. (1973). *Solid mechanics*. Springer.
[21] Atmane, H. A., Tounsi, A., Bernard, F. (2017). Effect of thickness stretching and porosity on mechanical response of a functionally graded beams resting on elastic foundations. *International Journal of Mechanics and Materials in Design*, 13(1):71–84.
[22] Chen, W. Q., Lü, C., Bian, Z. G. (2004). A mixed method for bending and free vibration of beams resting on a Pasternak elastic foundation. *Applied Mathematical Modelling*, 28(10):877–890.
[23] Ying, J., Lü, C., Chen, W. Q. (2008). Two-dimensional elasticity solutions for functionally graded beams resting on elastic foundations. *Composite Structures*, 84(3):209–219.